

Influence of Characteristic Energies and Charge Carriers Mobility on the Performance of a HIT Solar Cell

Wassila Leila Rahal^{1,*}, Djaaffar Rached^{2,†}

¹ Laboratoire d'Analyse et d'Application des Rayonnements, U.S.T.O.M.B. - B.P.,
1505 El M'naouar, Oran, Algérie

² Laboratoire de Physique des plasmas, Matériaux Conducteurs et leurs Applications, U.S.T.O.M.B. - B.P.,
1505 El M'naouar, Oran, Algérie

(Received 31 March 2017; revised manuscript received 25 July 2017; published online 27 July 2017)

In this article, two factors that limit the performance of HIT solar cells (Heterojunction with Intrinsic Thin layer) based on amorphous silicon / crystalline silicon are studied. First, we study the influence of the valence band tail width (characteristic energy ED) and the conduction band tail width (characteristic energy EA) of hydrogenated amorphous silicon [1]. Then we analyze the effect of electrons mobility μ_n and holes mobility μ_p in the emitter of the structure ITO/*p-a-Si:H* /*i-pm-Si:H* /*n-c-Si*/Al. Our results show that a decrease of ED in the *p-a-Si:H* layer decreases the donors density of states in the gap, as well as holes recombination in this layer. However, no amelioration is observed when EA decreases. Furthermore, we show that increasing the mobility of charge carriers μ_n and μ_p , enhance the performance of the studied solar cells.

Keywords: HIT solar cell, Amorphous silicon, Crystalline silicon, Characteristics energies, Band tails, Mobility, ASDMP.

DOI: [10.21272/jnep.9\(4\).04001](https://doi.org/10.21272/jnep.9(4).04001)

PACS numbers: 73.61.Jc, 71.20.Mq,
88.40.hj, 88.40.jj

1. INTRODUCTION

Recent years considerable progress has been achieved in the elaboration of solar cells [1, 2], though lot remains needed to reach better returns at lower cost. In the late 90s, the Japanese company Sanyo has started mass production of photovoltaic cell based HIT (Heterojunction with Intrinsic Thin layer) shown in Figure 1. By combining the good performance of crystalline silicon and low production cost of amorphous silicon, this technology allowed to reach high efficiencies while reducing the cost (lower thermal budget, thinner layers, which reduces the production cost) [3].

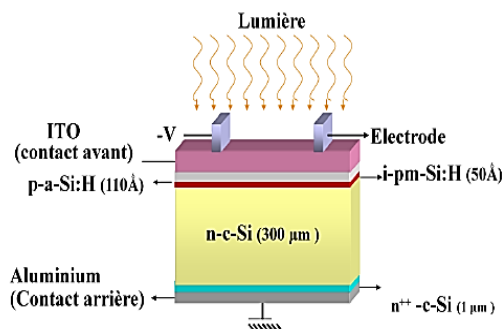


Fig. 1 – The heterostructure ITO/*p-a-Si:H*/*i-pm-Si:H*/*n-c-Si*/Al used in our simulations

The hydrogenated amorphous silicon present as thin layer in the HIT structure acts as the emitter of the solar cell. As in any amorphous semiconductor, there are localized states in the gap. These states come from the band tails (distortion of the crystal lattice) represented by exponential curves and

dangling-bonds represented by Gaussian. The distribution of these states determines many properties of the material, and greatly influences the performance of solar cells.

2. LOCALIZED STATES IN HYDROGENATED AMORPHOUS SILICON MIDGAP

In the amorphous silicon band diagram, states are extended in the valence and conduction bands, whereas they are located in the band tails that extend into the band gap.

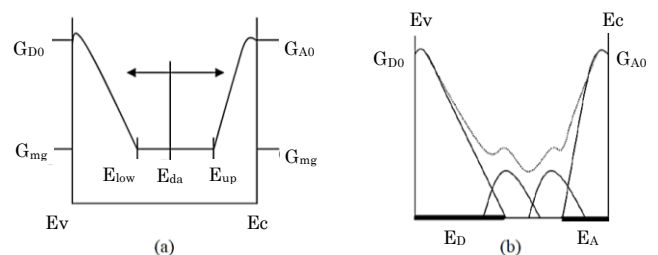


Fig. 2 – Density of band tail states in the forbidden band of hydrogenated amorphous silicon. (a) U-shaped model, (b) gaussian model

Deep defects due to the dangling bonds be modeled by two different distribution types: the U-shaped model (Figure 2a) and the Gaussian model (Figure 2b), both of which are integrated into the ASDMP software. In both cases, the donor and acceptor states in the strip tails have an exponential GDO and GAO prefactor. E_{da} is the energy at which the states pass from the donor to the acceptor type.

* wassilaleila@hotmail.com

† djaaffar31@yahoo.fr

2.1 Distribution Dans Les Queues de Bandes

The band tails of the donor states are modeled by Equation 1 [2]:

$$g_{DT}(E) = G_{D0} \exp[-E/E_D] \quad (1)$$

E is measured from E_v .

The band tails of the acceptor states are modeled by Equation 2:

$$g_{AT}(E') = G_{A0} \exp[-E'/E_A] \quad (2)$$

E' is measured from E_c . Value g represents the density of states D.O.S. ($\text{cm}^{-3} \text{eV}^{-1}$). E_D and E_A are the band tails characteristic energies.

2.2 Distribution in the Middle of the Gap

In the U -shaped model, the density of states in the gap is a constant value equal to G_{mg} (Fig. 2 (a)).

E_{up} and E_{low} are given by the equations 3 et 4:

$$E_{up} = E_A \cdot \ln(G_{A0}/G_{mg}) \quad (3)$$

$$E_{low} = E_D \cdot \ln(G_{D0}/G_{mg}) \quad (4)$$

E_{up} is measured from E_c . E_{low} is measured from E_v .

This flat region is added to the exponential region of the band tails for completing the U -shaped model.

In the Gaussian model, the distribution of the density of states in the mid-gap is modeled using two Gaussian distribution. In the case of hydrogenated amorphous silicon (a-Si:H), the separation between the two peaks of the two Gaussian distribution is equal to 0.5 eV [4, 8].

The first Gaussian consists of donor states ($D-/0$) of density of states $N_{AG} \text{ cm}^{-3}$. The second Gaussian distribution ($D+/0$) consists of acceptor states of density of states $N_{DG} \text{ cm}^{-3}$. The expressions of the density of states D.O.S are given in both cases by equations 5 and 6 [2].

$$g_{AG}(E'') = \left(\frac{N_{AG}}{\sqrt{2\pi} \sigma_{AG}} \right) \exp \left\{ -\frac{(E'' - E_{AG})^2}{2\sigma_{AG}^2} \right\} \quad (5)$$

$$g_{DG}(E''') = \left(\frac{N_{DG}}{\sqrt{2\pi} \sigma_{DG}} \right) \exp \left\{ -\frac{(E''' - E_{DG})^2}{2\sigma_{DG}^2} \right\} \quad (6)$$

Where E_{AG} and E_{DG} represent the two Gaussian peaks positions.

σ_{AG} and σ_{DG} represent the standard deviation of the two Gaussians.

The energies E'' and E''' are measured respectively from the peaks E_{AG} and E_{DG} .

3. SIMULATION MODEL

The different parameters of our device were determined by the ASDMP software [2, 4]. This

software was developed by Professor Parsathi Chatterjee. It is similar to the AMPS program [5-7] developed by Professor Fonash. The ASDMP model examines the behaviour of semiconductor device structures under steady state in one dimension by solving simultaneously Poisson's equation, the continuity equations for free electrons and the continuity equation for free holes using finite differences and the Newton-Raphson technique, and yields the Current-voltage $J(V)$ characteristics and the quantum efficiency [6, 7].

These equations are:

$$\frac{\partial^2 \Psi(x)}{\partial x^2} = \frac{\rho(x)}{\varepsilon} \quad (7)$$

$$G(x) - R(p(x), n(x)) - \frac{1}{q} \frac{\partial J_p(x)}{\partial x} = 0 \quad (8)$$

$$G(x) - R(p(x), n(x)) + \frac{1}{q} \frac{\partial J_n(x)}{\partial x} = 0 \quad (9)$$

$$\rho(x) = q [p(x) - n(x) + p_T(x) - n_T(x) + N_{net}^+] \quad (10)$$

$$E = \frac{\partial \Psi(x)}{\partial x} \quad (11)$$

In Poisson's equation (Eq.7), $\varepsilon(x)$ is the dielectric permittivity of the semiconductor. $\Psi(x)$ is the potential energy of an electron at the vacuum level in electron volts, and $\rho(x)$ is the space charge density in the semiconductor. In the continuity equations (Eq.8, Eq.9), $J_n(x)$ and $J_p(x)$ are the electron and hole current, respectively, and q is the charge of electron. The term $G_{net}(x)$ represents the net optical generation of free electron-hole pairs per unit volume, while $R_{net}(x)$ denotes the net recombination of free carriers per unit volume.

The generation term in the continuity equations has been calculated using a semiempirical model [8] that has been integrated into the modeling program. Both specular interference effects and diffused reflectances and transmittances due to interface roughness are taken into account.

The principal parameters used in this study are summarized in Table 1 [10, 11].

4. RESULTS AND DISCUSSIONS

First, we studied the sensitivity of the $J=f(V)$ characteristic, under illumination, to the E_D and E_A energies, which represent the characteristic energies of the band tails of the valence and conduction band of the amorphous silicon in the structure ITO/ p -a-Si:H / i - pm -Si:H / n - c -Si/Al.

In the ASDMP software, the tails of the donor states are modeled by the equation 12 [9]:

$$g_{DT}(E) = G_{D0} \exp[-E/E_D] \quad (12)$$

The tails of the acceptor states are modeled by the equation 13:

Table 1 – Principal input parameters

Parameters	<i>p-a-Si</i> :H	<i>i-pm-Si</i> :H	Defect layer <i>c-</i>	<i>n-c-Si</i>	BSF <i>n⁺⁺</i>
<i>d</i> (μm)	0.003-0.005	0.003	0.0032	299	1
χ (eV)	3.90	3.95	4.22	4.22	4.22
<i>E_a</i> (eV)	0.27	0.92	0.06	0.06	0.06
<i>E_μ</i> (eV)	1.90	1.96	1.12	1.12	1.12
<i>N_D</i> (cm ⁻³)	0	0	9·10 ¹⁴	9·10 ¹⁴	5·10 ¹⁸
<i>N_A</i> (cm ⁻³)	10 ¹⁹	0	0	0	0
<i>N_{DTOT}</i> , <i>N_{ATOT}</i> (cm ⁻³)	10 ¹⁹	10 ¹⁴	9·10 ¹⁴	3·10 ¹¹	3·10 ¹¹
<i>E_D</i> (eV)	0.050	0.050	0.050	0.005	0.005
<i>E_A</i> (eV)	0.030	0.030	0.030	0.003	0.003
<i>G_{DO}</i> , <i>G_{A0}</i> (cm ⁻³ eV ⁻¹)	4·10 ²¹	4·10 ²¹	10 ²⁰	10 ²⁰	10 ²⁰
μ_c (cm ² /V s)	20	30	1000	1000	1000
μ_{h+} (cm ² /V s)	4	12	450	450	450
<i>N_C</i> , <i>N_V</i>	2·10 ²⁰	2·10 ²⁰	5·10 ¹⁸	5·10 ¹⁸	5·10 ¹⁸
σ_n (cm ²)	10 ¹⁷	10 ¹⁷	10 ¹⁷	2·10 ¹⁹	2·10 ¹⁹
σ_c (cm ²)	10 ¹⁶	10 ¹⁶	10 ¹⁶	2·10 ¹⁸	2·10 ¹⁸
ϕ_{b0} (eV)	1,20				
ϕ_{bL} (eV)	0,06				

$$g_{AT}(E') = G_{A0} \exp[-E' / E_A] \quad (13)$$

Value *g* represents the density of states (D.O.S. (cm⁻³ eV⁻¹)).

We have represented the *J = f(V)* characteristic under illumination of the ITO/*p-a-Si*: H/*n-c-Si*/Al structure as a function of *E_D* in Figure 3 (a-d).

According to these graphs, we observe that when the characteristic energy *E_D* increases from 30 meV to 70 meV, the characteristic *J = f(V)* decreases, which results in the decrease of the photovoltaic parameters.

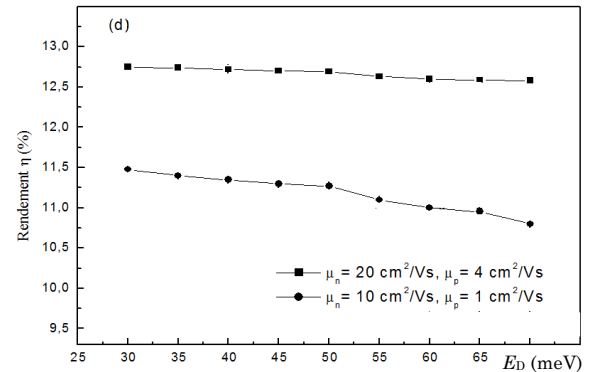
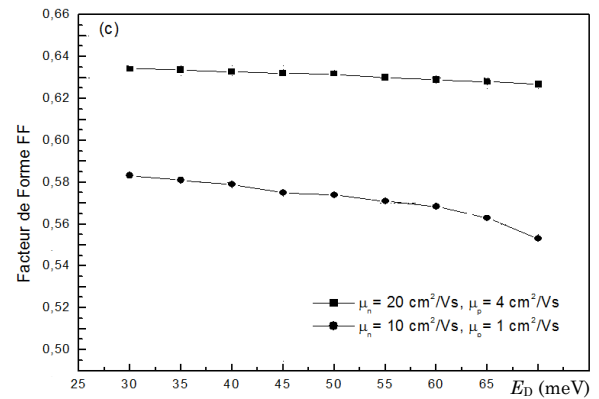
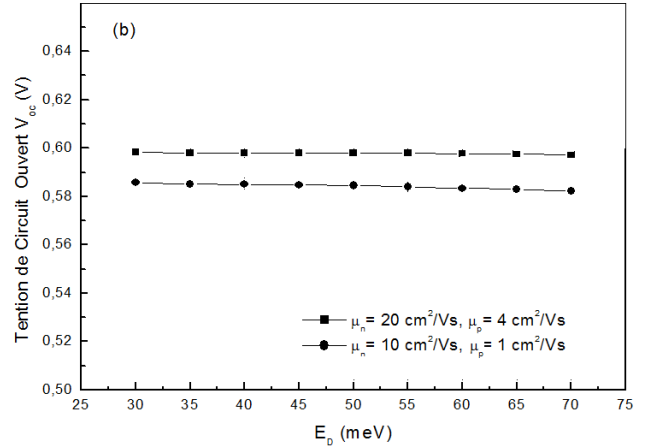
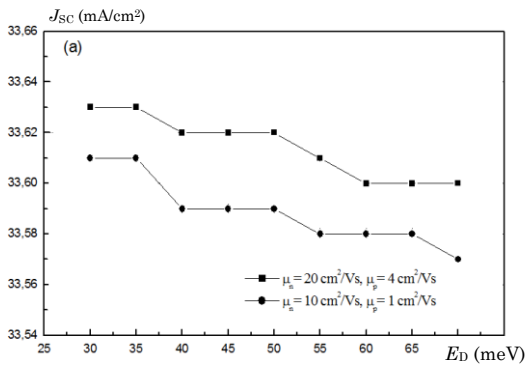


Fig.3 – Photovoltaic parameters of the ITO/*p-a-Si*:H/*i-pm-Si*:H/*n-c-Si* / Al structure as a function of *E_D*

This decrease is due to the increase of recombinations (Fig. 4a and b). An increase in *E_D* in the *p-a-Si*: H layer increases the donor states in the gap per unit volume, which explains this increase of recombinations.

On the other hand, we studied the influence of charge carriers mobilities on the photovoltaic parameters of the studied cell for *E_D* = 0.07 meV. We have found that when the electrons mobilities μ_n decrease from 20 cm² / Vs to 10 cm² / Vs and holes mobilities up from 4 cm² / Vs to 1 cm² / Vs, the *J = f(V)* characteristics decrease for the first *E_D* values. This leads to a reduction of the studied cells efficiency.

Graphs 3 and 4 respectively represent the

recombinations under illumination AM1.5 and the electric field in the depletion zone as a function of the position in the device and for mobilities μ_n of 20 cm²/Vs and 10 cm²/Vs and μ_p of 4 cm²/Vs and 1 cm²/Vs.

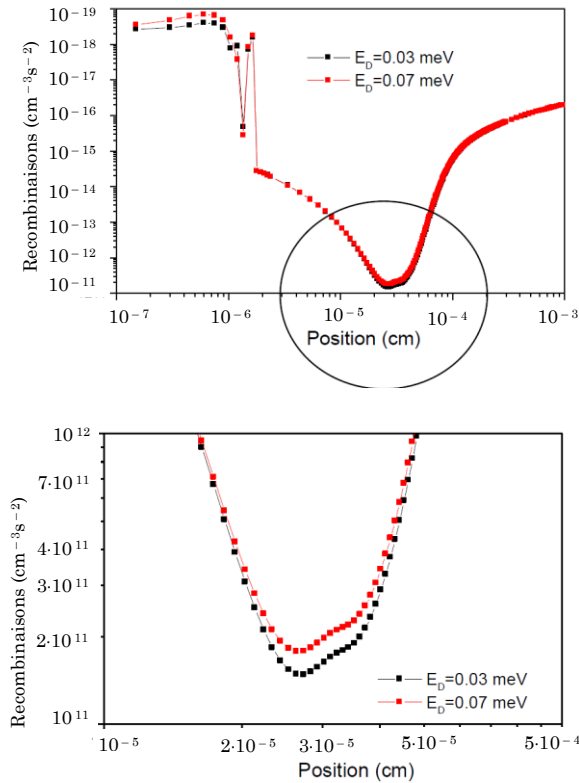


Fig.4 – Recombinations as a function of position in the structure ITO/*p-a-Si:H* /*i-pm-Si:H* /*n-c-Si/Al* under illumination AM1.5 for $E_D = 0.03$ meV and $E_D = 0.07$ meV.

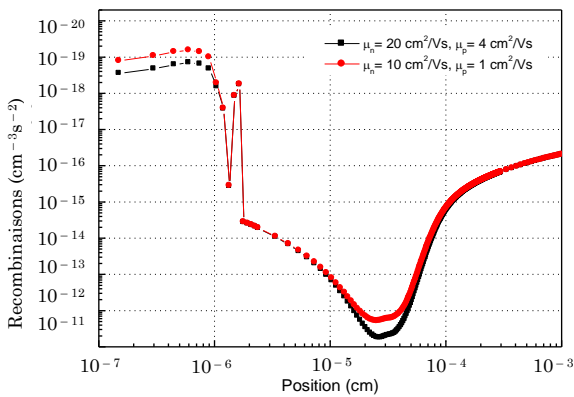


Fig. 5 – Recombinations as a function of position in the structure ITO/*p-a-Si:H* /*i-pm-Si:H* /*n-c-Si/Al* under illumination AM1.5 for $E_D = 0.07$ meV, electron mobility $\mu_n = 20$ cm²/Vs and 10 cm²/V, and the hole mobility $\mu_p = 4$ cm²/Vs and 1 cm²/Vs

We can see that the decrease of carrier mobility in the volume of the *p-a-Si:H* layer causes an increase in recombinations in the space charge area. We can conclude from graph 4 that this increase in recombinations is due to the increase of the electric field in the zone of space charge.

In the same way, we studied the variation of the

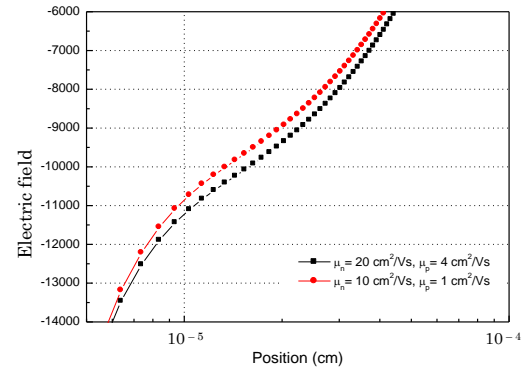


Fig.6 – The electric field in the depletion region depending on the position in the device for $E_D = 0.07$ meV, electron mobility $\mu_n = 20$ cm²/Vs and 10 cm²/V, and the hole mobility $\mu_p = 4$ cm²/Vs and 1 cm²/Vs

characteristic energy E_A . The height of the potential barrier ϕ_{b0} is taken equal to 1.20 eV. The characteristics $J = f(V)$ under illumination of the structure ITO/*p-a-Si:H* /*n-c-Si/Al* as a function of E_A remain unchanged. Indeed, an increase in E_A increases the acceptor states in the gap per unit volume, which implies an increase in the electrons recombinations of the *p-a-Si:H* layer which does not influence the holes collect.

We carried out a similar study for the same solar cells, ie n-type structures (ITO / *p-a-Si:H* / *i-pm-Si:H* / *n-c-Si/Al*) to check the behavior of these cells with respect to the characteristic energies E_D and E_A . We obtained the same results: an increase in the characteristic E_D energy as well as a decrease in the carriers mobilities, deteriorates the performances of the solar cells by a decrease in their characteristics while they remain unchanged for a variation of E_A .

5. CONCLUSION

In this work, we have shown that in order to obtain a good quality of photovoltaic HIT cells, it is important to reduce the characteristic energy of the conduction band tail E_D in order to reduce the rate of recombination of the holes in the *p-a-Si:H* layer and thus increase the efficiency of the studied cells. We have also come to the conclusion that the modification of the energy characteristic E_A of the valence band does not influence the quality of the cells.

On the other hand, we have observed that when the electrons mobility μ_n decreases from 20 cm²/Vs to 10 cm²/Vs and holes mobility μ_p from 4 cm²/Vs to 1 cm²/Vs, all photovoltaic parameters of the studied Cell decrease.

ACKNOWLEDGEMENTS

We would be thankful to Prof. Pere Rocas I Cabarrocas, research director at LPICM, Ecole Polytechnique, Palaiseau France and Prof. P.Chatterjee, Energy Research Unit, Indian Association for the Cultivation of Science, Kolkata 700 032, India, for their help and benefits discussions.

REFERENCES

1. Y. Poissant, P. Chatterjee, P. R. Cabarrocas, *J. Appl. Phys.* **93** No 4, 170 (2003).
2. P. Chatterjee, M. Favre, F. Leblanc, J. Perrin, *Mater. Res. Soc. Symp. Proc.* **426**, 593 (1996).
3. V.A. Dao, *Current Photovoltaic Research* **1** No 2, 73 (2013).
4. N. Palit, P. Chatterjee, *Sol. Energy Mater. Sol. C.* **53**, 235 (1998).
5. P.J. McElheny, J.K. Arch, H.-S. Lin, S.J. Fonash, *J. Appl. Phys.* **64**, 1254 (1988).
6. P. Chatterjee, *J. Appl. Phys.* **76** No 2, 1301 (1994).
7. P. Chatterjee, *J. Appl. Phys.* **79** No 9, 7339 (1996).
8. F. Leblanc, J. Perrin, J. Schmitt, *J. Appl. Phys.* **75**, 1074 (1994).
9. B.M. Omer, *Chin. Phys. Lett.* **32** No 8, 088801 (2015).
10. D. Rached, M. Mostefaoui, *Thin Solid Films* **516**, 5087 (2008).
11. D. Rached, H.M. Yssad, *Acta Phys. Pol. A* **127** No 3, 767 (2015).